SMART GRID-REINFORCED COMPOSITE STRUCTURES: MICROMECHANICS AND EFFECTIVE PROPERTIES

Alexander L. Kalamkarov, alex.kalamkarov@dal.ca
Department of Mechanical Engineering, Dalhousie University, Halifax, Nova Scotia, B3J 2X4, Canada

Marcelo A. Savi, savi@mecanica.ufrj.br
Department of Mechanical Engineering, COPPE, Universidade Federal do Rio de Janeiro, Rio de Janeiro, RJ, Brazil

Abstract. *A comprehensive micromechanical model for smart 3D composite structures reinforced by a periodic grid of orthotropic cylindrical reinforcements that also exhibit piezoelectric behavior is presented. The derivation is based on the application of the multi-scale asymptotic homogenization method. The model assumes that the constituents (actuators and reinforcements) are made of generally orthotropic materials. By means of the solution of the unit cell problems the analytical expressions for the effective elastic and piezoelectric coefficients of the homogenized smart 3D grid-reinforced composites are obtained. The developed model is applied to different examples of smart orthotropic composite structures with cubic, conical and diagonal arrangement of actuators and reinforcements.*

Keywords: *Smart 3D grid-reinforced composite, Asymptotic homogenization, Effective piezoelastic properties.*

1. INTRODUCTION

Composite structures have recently entered new branches of engineering applications owing, in part, to the technological innovations appearing in other fields such as physics and telecommunications which have developed novel and highly efficient sensors and actuators. The integration of these sensors and actuators with structural composites gave birth to smart composite structures. As a consequence of the microstructural makeup of smart composites, effective formulation of the pertinent micromechanical models must take into consideration both local and global aspects and characteristics. Accordingly, the developed models should be rigorous enough to enable the consideration of the spatial distribution, mechanical properties, and behavior of the different constituents (reinforcing elements, matrix, actuators, sensors etc) at the local level, but, not too complex to be described and used via straightforward analytical and numerical approaches.

A very effective technique that can be used for the analysis of smart composites with regular structures is the asymptotic homogenization method. A complete mathematical framework of asymptotic homogenization method can be found in Sanchez-Palencia (1980), Bakhvalov & Panasenko (1989), and Kalamkarov (1992).This method is mathematically rigorous and it enables the prediction of both the local and global effective properties of the composite structure. Many problems in the framework of elasticity and thermoelasticity have been solved using such models, see for example, Kalamkarov (1992), Kalamkarov & Kolpakov (1997,2001), Kalamkarov & Georgiades (2002a,2002b,2004). More recently, Kalamkarov et al. (2006), Georgiades et al. (2006) and Challagulla et al. (2007, 2008) have determined effective coefficients of the grid-reinforced composite plates and shells. Saha & Kalamkarov (2009), Saha et al. (2007a,2007b) investigated composite sandwich shells made of generally orthotropic materials.

The present study aims to develop comprehensive micromechanical model for smart 3D grid-reinforced composite structures with embedded orthotropic reinforcements that may exhibit piezoelectric behavior. The model assumes that the

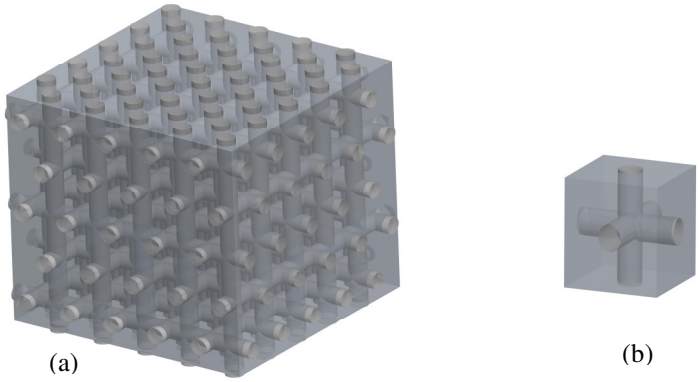

Figure 1. (a) 3D grid-reinforced smart composite structure S_1, (b) its unit cell

constituents of composite structure (reinforcement/actuators) are made of generally orthotropic materials and this renders the pertinent mathematical analysis much more complicated. The formulated models are subsequently used to evaluate the effective elastic and piezoelectric coefficients of such structures, see, i.g., Fig. 1. The derived micromechanical models are applied to several examples involving smart composite structures with embedded cubic, conical and diagonal arrangements of reinforcements/ actuators.

Following this introduction the rest of the paper is organized as follows: The basic problem formulation is presented in Section 2. Sections 3 and 4 are dedicated to the development of the general piezoelastic model pertaining to smart 3D grid-reinforced composite structures with orthotropic reinforcements/actuators. Several practically-important examples are considered in the Section 5.

2. ASYMPTOTIC HOMOGENIZATION MODEL FOR 3D COMPOSITE STRUCTURES

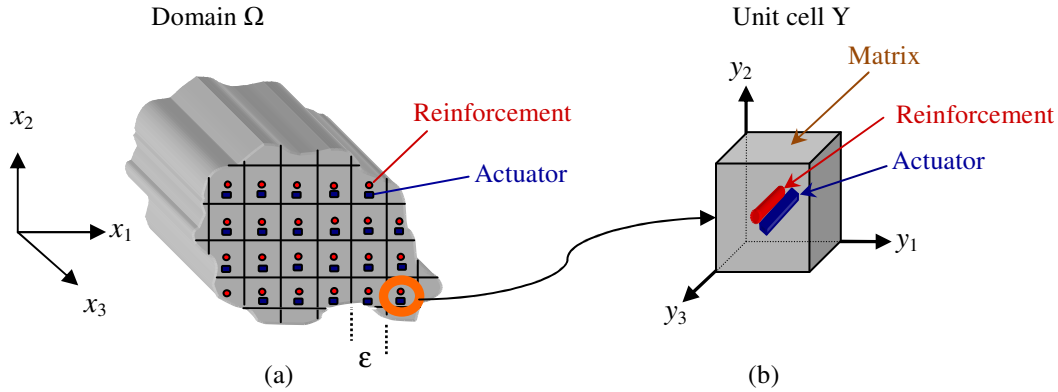

Figure 2. (a) 3D smart composite solid of a regular structure, (b) unit cell Ω_δ.

Consider a smart composite structure representing an inhomogeneous solid occupying domain Ω with boundary $\partial\Omega$ that contains a large number of periodically arranged reinforcements and actuators as shown in Fig. 2(a). It can be observed that this periodic structure is obtained by repeating a small unit cell Y in the domain Ω, see Fig. 2(b).

The elastic deformation of this structure can be described by means of the following boundary-value problem:

$$\frac{\partial \sigma_{ij}}{\partial x_j} = f_i \quad in\ \Omega, \qquad u_i(\boldsymbol{x}) = 0 \quad on\ \partial\Omega, \tag{1}$$

$$\sigma_{ij} = C_{ijkl} e_{kl} - P_{ijk} R_k(\boldsymbol{x}), \qquad e_{ij} = \frac{1}{2}\left(\frac{\partial u_i}{\partial x_j} + \frac{\partial u_j}{\partial x_i}\right) \tag{2}$$

In Eqs. (1),(2) and in the sequel all indices assume values of 1, 2, 3 and the summation convention is adopted, C_{ijkl} is the tensor of elastic coefficients, e_{kl} is the strain tensor which is a function of the displacement field u_i, P_{ijk} is a tensor of piezoelectric coefficients describing the effect of a control signal $\boldsymbol{R}$ on the stress field σ_{ij}. Finally, f_i represent body forces. It is assumed in Eq. (1) that all the elastic and piezoelectric coefficients are periodic with a unit cell Y of characteristic dimension ε. Small parameter ε is made non-dimensional by dividing the size of the unit cell by a certain characteristic dimension of the overall structure.

The development of asymptotic homogenization model for the 3D smart composite structures can be found in Kalamkarov (1992), Kalamkarov et al. (2009a). In this Section, only a brief overview of the steps involved in the development of the model are given in so far as it represents the starting point of our current work. The first step is to define the so-called "fast" or microscopic variables according to:

$$y_1 = x_1 / \varepsilon, \quad y_2 = x_2 / \varepsilon, \quad y_3 = x_3 / \varepsilon \tag{3}$$

As a consequence of introducing $\boldsymbol{y}$, the derivatives are also transformed according to

$$\frac{\partial}{\partial x_1} \to \frac{\partial}{\partial x_1} + \frac{1}{\varepsilon}\frac{\partial}{\partial y_1}, \quad \frac{\partial}{\partial x_2} \to \frac{\partial}{\partial x_2} + \frac{1}{\varepsilon}\frac{\partial}{\partial y_2}, \quad \frac{\partial}{\partial x_3} \to \frac{\partial}{\partial x_3} + \frac{1}{\varepsilon}\frac{\partial}{\partial y_3} \tag{4}$$

The boundary value problem and corresponding stress field defined in Eqs. (1) and (2) are thus readily transformed into the following expressions:

$$\frac{\partial \sigma_{ij}(\boldsymbol{x},\boldsymbol{y})}{\partial x_j} + \frac{1}{\varepsilon}\frac{\partial \sigma_{ij}(\boldsymbol{x},\boldsymbol{y})}{\partial y_i} = f_i \ \ in\ \Omega, \quad u_i(\boldsymbol{x},\boldsymbol{y}) = 0 \quad on\ \partial\Omega \tag{5}$$

$$\sigma_{ij}(\boldsymbol{x},\boldsymbol{y}) = C_{ijkl}(\boldsymbol{y})\frac{\partial u_k}{\partial x_l}(\boldsymbol{x},\boldsymbol{y}) - P_{ijk}(\boldsymbol{y})R_k(\boldsymbol{x}) \tag{6}$$

The next step is to consider the following asymptotic expansions in terms of powers of the small parameter ε:

$$u_i(\boldsymbol{x},\boldsymbol{y}) = u_i^{(0)}(\boldsymbol{x},\boldsymbol{y}) + \varepsilon u_i^{(1)}(\boldsymbol{x},\boldsymbol{y}) + \varepsilon^2 u_i^{(2)}(\boldsymbol{x},\boldsymbol{y}) + \ldots \tag{7}$$

$$\sigma_i(\boldsymbol{x},\boldsymbol{y}) = \sigma_i^{(0)}(\boldsymbol{x},\boldsymbol{y}) + \varepsilon \sigma_i^{(1)}(\boldsymbol{x},\boldsymbol{y}) + \varepsilon^2 \sigma_i^{(2)}(\boldsymbol{x},\boldsymbol{y}) + \ldots \tag{8}$$

By substituting Eqs. (7),(8) into Eqs. (5),(6) and considering at the same time the periodicity of $\boldsymbol{u}^{(i)}$ in $\boldsymbol{y}$ one can readily eliminate the microscopic variable $\boldsymbol{y}$ from the first term $\boldsymbol{u}^{(0)}$ in the asymptotic displacement field expansion thus showing that it depends only on the macroscopic variable $\boldsymbol{x}$. Subsequently, by separating terms with like powers of ε one obtains a series of differential equations the first two of which are:

$$\frac{\partial \sigma_{ij}^{(0)}}{\partial y_j} = 0, \quad \frac{\partial \sigma_{ij}^{(1)}}{\partial y_j} + \frac{\partial \sigma_{ij}^{(0)}}{\partial x_j} = f_i \tag{9}$$

where

$$\sigma_{ij}^{(0)} = C_{ijkl}\left(\frac{\partial u_k^{(0)}}{\partial x_l} + \frac{\partial u_k^{(1)}}{\partial y_l}\right) - P_{ijk}R_k, \quad \sigma_{ij}^{(1)} = C_{ijkl}\left(\frac{\partial u_k^{(1)}}{\partial x_l} + \frac{\partial u_k^{(2)}}{\partial y_l}\right) \tag{10}$$

Combination of Eq. (9) and Eq. (10) leads to the following expression:

$$\frac{\partial}{\partial y_j}\left(C_{ijkl}\frac{\partial u_k^{(1)}(\boldsymbol{x},\boldsymbol{y})}{\partial y_l}\right) = \frac{\partial P_{ijk}(\boldsymbol{y})}{\partial y_j}R_k(\boldsymbol{x}) - \frac{\partial C_{ijkl}(\boldsymbol{y})}{\partial y_j}\frac{\partial u_k^{(0)}(\boldsymbol{x})}{\partial x_l} \tag{11}$$

The separation of variables in the right-hand-side of Eq. (11) prompts us to represent the solution for $\boldsymbol{u}^{(1)}$ as:

$$u_m^{(1)}(\boldsymbol{x},\boldsymbol{y}) = \frac{\partial u_k^{(1)}(\boldsymbol{x})}{\partial x_l}N_m^{kl}(\boldsymbol{y}) + R_k(\boldsymbol{x})N_m^k(\boldsymbol{y}) \tag{12}$$

where the auxiliary functions N_m^{kl} and N_m^k are periodic in $\boldsymbol{y}$ and they satisfy the following problems:

$$\frac{\partial}{\partial y_j}\left(C_{ijmn}(\boldsymbol{y})\frac{\partial N_m^{kl}(\boldsymbol{y})}{\partial y_n}\right) = -\frac{\partial C_{ijkl}}{\partial y_j} \tag{13}$$

$$\frac{\partial}{\partial y_j}\left(C_{ijmn}(\boldsymbol{y})\frac{\partial N_m^{k}(\boldsymbol{y})}{\partial y_n}\right) = \frac{\partial P_{ijk}}{\partial y_j} \tag{14}$$

One observes that Eqs. (13) and (14) depend only on the fast variable $\boldsymbol{y}$ and thus are formulated in the domain Y of the unit cell, remembering at the same time that all of C_{ijkl}, P_{ijk} and N_m^{kl} and N_m^k are Y-periodic in $\boldsymbol{y}$. Consequently, Eqs. (13) and (14) are appropriately called the unit-cell problems.

The next important step in the model development is the homogenization procedure. This is carried out by first substituting Eq. (12) into Eq. (10), and combining the result with Eq. (9). The resulting expressions are then integrated over the unit cell Y (with the volume $|\mathrm{Y}|$) remembering to treat $\boldsymbol{x}$ as a parameter as far as integration with respect to $\boldsymbol{y}$ is concerned. After canceling out terms that vanish due to periodicity this yields

$$\tilde{C}_{ijkl}\frac{\partial^2 u_k^{(0)}(\boldsymbol{x})}{\partial x_j \partial x_l} - \tilde{P}_{ijk}\frac{\partial R_k(\boldsymbol{x})}{\partial x_j} = f_i \tag{15}$$

where the following definitions are introduced:

$$\tilde{C}_{ijkl} = \frac{1}{|Y|}\int_Y \left(C_{ijkl}(\boldsymbol{y}) + C_{ijmn}(\boldsymbol{y})\frac{\partial N_m^{kl}(\boldsymbol{y})}{\partial y_n}\right)\mathrm{dv} \tag{16}$$

$$\tilde{P}_{ijk} = \frac{1}{|Y|}\int_Y \left(P_{ijk}(\boldsymbol{y}) - C_{ijmn}(\boldsymbol{y})\frac{\partial N_m^{k}(\boldsymbol{y})}{\partial y_n}\right)\mathrm{dv} \tag{17}$$

Coefficients $\tilde{C}_{ijkl}, \tilde{P}_{ijk}$ defined by Eqs. (16),(17) are the effective elastic and piezoelectric coefficients respectively. It is noticed that all the effective coefficients are constant unlike of their original rapidly varying material counterparts C_{ijkl}, P_{ijk} and therefore problem (15) is much simpler than the original problem (5),(6). The effective coefficients shown above are universal in nature and can be used to study a wide variety of boundary value problems associated with a given composite structure. It is worth mentioning at this point that although the present work pertains to piezoelectric actuators, the model derived applies equally well if the smart composite structure is associated with some general transduction properties that can be used to induce residual strains and stresses. In that case, the coefficients $\tilde{P}_{ijk}$ represent the appropriate effective actuation coefficients (rather than the piezoelectric ones).

In summary, Eqs. (13)-(17) represent the governing equations of the homogenized model for a smart composite structure with periodically arranged reinforcements and actuators. Eqs. (13),(14) represent the unit cell problems, formulae (16),(17) define the effective properties, and Eq. (15) defines the displacement field.

3. 3D SMART GRID-REINFORCED COMPOSITE STRUCTURES

In the subsequent Sections we will consider the problem of a smart 3D composite structure reinforced with *N* families of reinforcements/actuators, see for instance Fig. 1 where an explicit case of multiple families of reinforcements is shown. We assume that the members of each family are made of different generally orthotropic materials that may exhibit piezoelectric characteristics and that the reinforcements of each family make angles $\varphi_1^n, \varphi_2^n, \varphi_3^n$ ($n = 1, 2, ..., N$) with the y_1, y_2, y_3 axes respectively. It is further assumed that the orthotropic reinforcements/actuators have significantly larger elastic moduli than the matrix material, so we are justified in neglecting the contribution of the matrix phase in the ensuing analytical treatment. Clearly, for the particular case lattice grid structures the surrounding matrix is absent and this is modeled by assuming zero matrix rigidity.

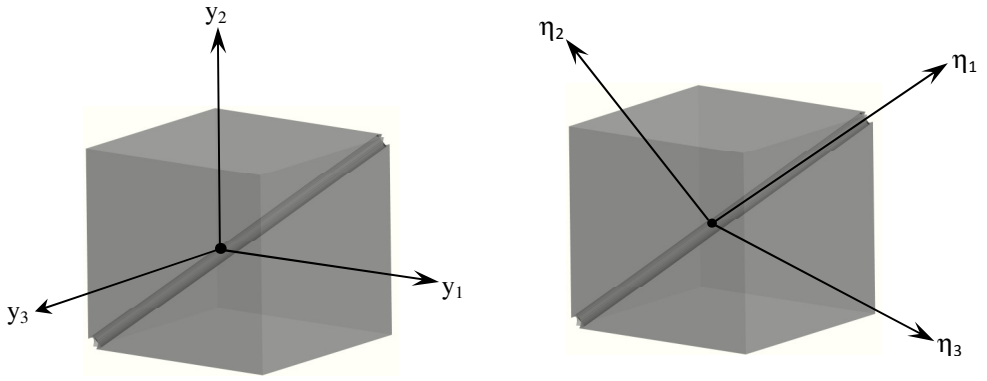

Figure 3. Unit cell in case of a single reinforcement family in original and rotated microscopic coordinates.

The nature of the grid-reinforced composite structure of Fig. 1 is such that it would be more efficient if we first considered a simpler type of unit cell made of only a single reinforcement/actuator as shown in Fig. 3. Having dealt with this situation, the effective elastic and piezoelectric coefficients of more general structures with multiple families of reinforcements/actuators can be determined by superposition of the solution for each of them found separately. In following this procedure, one must naturally accept the error incurred at the regions of intersection between the reinforcements. However, our approximation will be quite accurate since these regions of intersection are very localized and do not contribute significantly to the integral over the entire volume of the unit cell. Essentially, the error incurred will be negligible if the dimensions of the actuators/reinforcements are much smaller than the spacing between them. The mathematical justification for this argument in the form of the so-called principle of the split homogenized operator can be found in Bakhvalov & Panasenko (1989).

In order to calculate the effective coefficients for the simpler smart structure of Fig. 3, unit cell problems given by Eqs. (13) and (14) must be solved and, subsequently, Eqs. (16) and (17) must be applied.

The problem formulation for the structure shown in Fig. 3 begins with the introduction of the following local functions:

$$b_{ij}^{kl} = C_{ijkl}(\boldsymbol{y}) + C_{ijmn}(\boldsymbol{y}) \frac{\partial N_m^{kl}(\boldsymbol{y})}{\partial y_n} \tag{18}$$

$$b_{ij}^{k} = P_{ijk}(\mathbf{y}) - C_{ijmn}(\mathbf{y})\frac{\partial N_m^k(\mathbf{y})}{\partial y_n} \tag{19}$$

The unit cell problems in Eqs. (13), (14) can be then written as follows:

$$\frac{\partial}{\partial y_j} b_{ij}^{kl} = 0, \qquad \frac{\partial}{\partial y_j} b_{ij}^{k} = 0 \tag{20}$$

Perfect bonding conditions are assumed at the interfaces between the actuators/reinforcements and the matrix. This assumption yields the following interface conditions:

$$N_n^{kl}(r)\big|_s = N_n^{kl}(m)\big|_s, \; b_{ij}^{kl}(r)n_j\big|_s = b_{ij}^{kl}(m)n_j\big|_s \tag{21}$$

$$N_n^{k}(r)\big|_s = N_n^{k}(m)\big|_s, \quad b_{ij}^{k}(r)n_j\big|_s = b_{ij}^{k}(m)n_j\big|_s \tag{22}$$

In Eqs. (21), (22) "*r*", "*m*", and "*s*" denote the "actuator/reinforcement", "matrix", and reinforcement/matrix interface, respectively; while n_j denote the components of the unit normal vector at the interface. As was mentioned earlier, we will further assume that $C_{ijkl}(m) = 0$ which implies from Eqs. (18),(19) that $b_{ij}^{kl}(m) = b_{ij}^{k}(m) = 0$. Therefore, the interface conditions in Eqs. (21),(22) become:

$$b_{ij}^{kl}(r)n_j\big|_s = 0, \qquad b_{ij}^{k}(r)n_j\big|_s = 0 \tag{23}$$

In summary, the unit cell problems that must be solved for the 3D grid-reinforced smart composite structure with a single family of orthotropic reinforcements/actuators are given by Eqs. (18)-(20) in conjunction with Eqs. (21)-(23).

In order to solve the pertinent unit cell problems we perform a coordinate transformation of the global coordinate system $\{y_1, y_2, y_3\}$ into the new coordinate system $\{\eta_1, \eta_2, \eta_3\}$ shown in Fig. 3. With the new coordinate system we note that since the reinforcement is oriented along the η_1 coordinate axis, the problem at hand becomes independent of η_1 and depend only on η_2 and η_3. As a result, the ensuing analysis becomes much easier.

4. EFFECTIVE ELASTIC AND PIEZOELECTRIC COEFFICIENTS

A scheme for the determination of the effective elastic coefficients for 3D grid-reinforced composite structures with generally orthotropic reinforcements is given in detail in Kalamkarov et al. (2009b). It is noteworthy to mention that in the limiting particular case of 2D grid-reinforced structure with isotropic reinforcements the developed expressions for these coefficients converge to those obtained earlier by Kalamkarov (1992).

With reference to Fig. 3, we begin by rewriting Eqs. (18),(23) in the $\{\eta_1, \eta_2, \eta_3\}$ coordinates to get:

$$\mathrm{b_{ij}^{kl}} = \mathrm{C_{ijkl}}(\mathbf{y}) + \mathrm{C_{ijmn}q_{pn}}\frac{\partial \mathrm{N_m^{kl}}(\mathbf{y})}{\partial \eta_p}, \quad \left(\mathrm{b_{ij}^{kl}q_{2j}n_2^{'}}(r) + \mathrm{b_{ij}^{kl}q_{3j}n_3^{'}}(r)\right)\Big|_s = 0 \tag{24}$$

Here, $n_2^{'}$ and $n_3^{'}$ are the components of the unit normal vector in the new coordinate system. Expanding Eq. (24) and keeping in mind the independency of the unit cell problem on η_1 yields:

$$\mathrm{b_{ij}^{kl}} = \mathrm{C_{ijkl}} + \mathrm{C_{ijm1}q_{21}}\frac{\partial \mathrm{N_m^{kl}}}{\partial \eta_2} + \mathrm{C_{ijm2}q_{22}}\frac{\partial \mathrm{N_m^{kl}}}{\partial \eta_2} + \mathrm{C_{ijm3}q_{23}}\frac{\partial \mathrm{N_m^{kl}}}{\partial \eta_2} + \mathrm{C_{ijm1}q_{31}}\frac{\partial \mathrm{N_m^{kl}}}{\partial \eta_3} + \mathrm{C_{ijm2}q_{32}}\frac{\partial \mathrm{N_m^{kl}}}{\partial \eta_3} + \mathrm{C_{ijm3}q_{33}}\frac{\partial \mathrm{N_m^{kl}}}{\partial \eta_3} \tag{25}$$

Apparently, Eqs. (24),(25) can be solved by assuming a linear variation of the local functions N_m^{kl} with respect to η_2 and η_3:

$$\mathrm{N_1^{kl}} = \lambda_1^{kl}\eta_2 + \lambda_2^{kl}\eta_3, \;\; \mathrm{N_2^{kl}} = \lambda_3^{kl}\eta_2 + \lambda_4^{kl}\eta_3, \;\; \mathrm{N_3^{kl}} = \lambda_5^{kl}\eta_2 + \lambda_6^{kl}\eta_3, \tag{26}$$

where λ_i^{kl} are constants to be determined from the boundary conditions. Once these coefficients are determined, the coefficients b_{ij}^{kl} are found from the Eq. (25). In turn, these are used to calculate the effective elastic coefficients of the structure of Fig. 3 by integrating over the volume of the unit cell:

$$\tilde{\mathrm{C}}_{\mathrm{ijkl}} = \frac{1}{|\mathrm{Y}|}\int_{\mathrm{Y}} \mathrm{b_{ij}^{kl}}\,\mathrm{dv} \tag{27}$$

Noting that b_{ij}^{kl} are constants, the effective elastic coefiicients become

$$\tilde{\mathrm{C}}_{\mathrm{ijkl}} = \mu_f\,\mathrm{b_{ij}^{kl}} \tag{28}$$

where μ_f is the volume fraction of the reinforcement within the unit cell. It can be proved in general case that the effective elastic coefficients $\tilde{C}_{ijkl}$ maintain the same symmetry and convexity properites as their actual material counterparts C_{ijkl}, see Kalamkarov (1992).

The above derived effective moduli pertain to grid-reinforced structures with a single family of reinforcements. For structures with more than one family of reinforcements the effective moduli can be obtained by superposition. The effective elastic coefficients of a grid-reinforced structure with *N* families of generally orthotropic reinforcements will be given by:

$$\tilde{C}_{ijkl} = \sum_{n=1}^{N} V \mu_f^{(n)} b_{ij}^{(n)kl} \tag{29}$$

where the superscript *(n)* represents the *n-th* reinforcement family with the reinforcement volume fraction $\mu_f^{(n)}$.

Let us now proceed to calculation of the effective piezoelectric coefficients from the unit cell problem given by the Eqs. (19),(22),(23) which in coordinates $\{\eta_1, \eta_2, \eta_3\}$ becomes

$$b_{ij}^k = P_{ijk} - C_{ijmn} q_{pn} \frac{\partial N_m^k}{\partial \eta_p}, \quad \left(b_{ij}^k q_{2j} n_2'(r) + b_{ij}^k q_{3j} n_3'(r) \right)\Big|_s = 0 \tag{30}$$

Keeping in mind independency on η_1, Eq. (30) yields:

$$b_{ij}^k = P_{ijk} - \left(C_{ijm1} q_{21} \frac{\partial N_m^k}{\partial \eta_2} + C_{ijm2} q_{22} \frac{\partial N_m^k}{\partial \eta_2} + C_{ijm3} q_{23} \frac{\partial N_m^k}{\partial \eta_2} + C_{ijm1} q_{31} \frac{\partial N_m^k}{\partial \eta_3} + C_{ijm2} q_{32} \frac{\partial N_m^k}{\partial \eta_3} + C_{ijm3} q_{33} \frac{\partial N_m^k}{\partial \eta_3} \right) \tag{31}$$

It can be shown that the Eq. (31) in conjunction with the Eq. (30) can be solved by assuming a linearity of functions $N_m^k(\boldsymbol{y})$ in η_2 and η_3:

$$N_1^k = \Sigma_1^k \eta_2 + \Sigma_2^k \eta_3, \quad N_2^k = \Sigma_3^k \eta_2 + \Sigma_4^k \eta_3, \quad N_3^k = \Sigma_5^k \eta_2 + \Sigma_6^k \eta_3, \tag{32}$$

where Σ_i^k are constants that can be determined from the boundary conditions. The functions (33), (34) are used to calculate the effective piezolectric coefficients of the smart composite structure of Fig. 3 by integrating over the volume of the unit cell, which on account of Eqs. (17),(19) yields

$$\tilde{P}_{ijk} = = \frac{1}{|Y|} \int_Y b_{ij}^k dv \tag{33}$$

Since the local functions b_{ij}^k are constant, the effective piezoelectric coefficients become

$$\tilde{P}_{ijk} = \mu_f b_{ij}^k \tag{34}$$

where μ_f is the volume fraction of the actuators/reinforcement within the unit cell.

The effective piezolectric coefficients derived above pertain to grid-reinforced smart composite structures with a single family of actuators/reinforcements (or inclusions in general inlusions). For structures with multiple families of inlusions the effective actuation coefficients can be obtained by superimposition. For instance, pertaining to a grid-reinforced smart composite structure with *N* families of actuators/reinforcements the effective coefficients will be given by

$$\tilde{P}_{ijk} = \sum_{n=1}^{N} \mu_f^{(n)} b_{ij}^{(n)k}, \tag{35}$$

where the superscript (*n*) represents the n^{th} reinforcement/actuator family, as in the above Eq. (29).

5. EXAMPLES OF SMART GRID-REINFORCED COMPOSITE STRUCTURES

The developed micromechanical model will now be used to analyze three different practically important examples of smart 3D grid-reinforced composite structures with orthotropic actuators/reinforcements. The first example, structure S_1 is shown in Fig. 1. It has three families of orthotropic actuators/reinforcements, each family oriented along one of the coordinate axes. The second example, structure S_2 is shown in Fig. 4. It is formed by a conical array of orthotropic reinforcements/actuators. And the third example, structure S_3 is shown in Fig. 5. It has a unit cell formed by three actuators/reinforcements, two of them extended diagonally across the unit cell between two diametrically opposite vertices while the third reinforcement is spun between the middles of the bottom edge and the top edge on the opposite face.

The effective elastic and piezoelectric coefficients for the above introduced structures are calculated on the basis of Eqs. (29),(35). Although the obtained analytical results are too lengthy to be reproduced here, the plots of some of these

effective coefficients will be shown below, see Kalamkarov et al. (2009b) and Hassan et al. (2011) for the details. We assume that the actuators/reinforcements are made of piezoelastic material PZT-5A with the following material properties (Cote et al., 2002): $C_{11}^{(p)} = C_{22}^{(p)} = 121.0\,\text{GPa},\ C_{33}^{(p)} = 111.0\,\text{GPa}, C_{12}^{(p)} = 75.4\,\text{GPa}, C_{13}^{(p)} = C_{23}^{(p)} = 75.2\text{GPa}, C_{44}^{(p)} = 22.6\,\text{GPa},$ $C_{55}^{(p)} = C_{66}^{(p)} = 21.1\ \text{GPa},\ P_{13}^{(p)} = P_{23}^{(p)} = -5.45\times10^{-6}\,\text{C/mm}^2, P_{33}^{(p)} = 1.56\times10^{-5}\,\text{C/mm}^2, P_{42}^{(p)} = P_{51}^{(p)} = 2.46\times10^{-5}\,\text{C/mm}^2.$

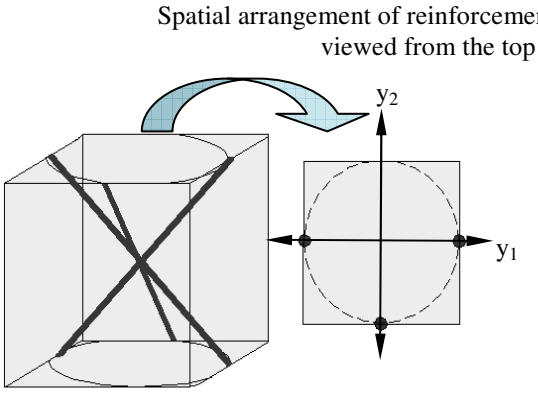

Figure 4. Unit cell of smart composite structure S_2 with conical arrangement of orthotropic reinforcements/actuators

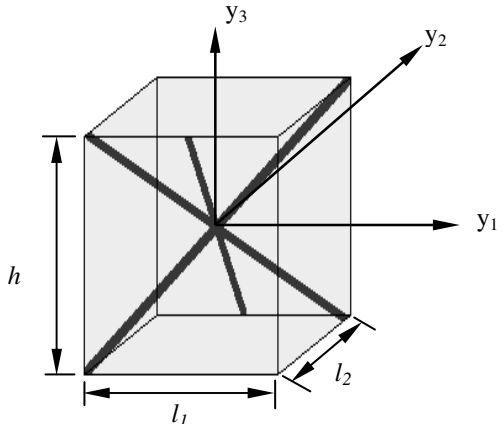

Figure 5. Unit cell of smart composite structure S_3 with diagonally arranged orthotropic actuators/reinforcements

We start with the structure S_1 shown in Fig. 1. Typical piezoelectric coefficients are plotted vs. volume fraction in Fig. 6. As expected, these coefficients increase in magnitude as the volume fraction increases. One also observes from Fig. 6 that the values of $\tilde{P}_{333}$ are larger than $\tilde{P}_{113}$ for a given volume fraction, which is to be expected because the former refers to the stress response in the direction y_3 in which the electric field is applied.

We now turn our attention to structure S_2 of Fig. 4. Typical effective piezoelectric coefficients are plotted vs. the total volume fraction of the actuators/reinforcements within the unit cell in Figs. 7 and 8. As expected, the plots show an increase in the effective piezoelectric coefficients as the overall volume fraction increases. And it is seen from the Figs. 6 and 7 that the magnitude of the coefficient $\tilde{P}_{113}$ (which refers to the stress response of the structure in the y_1-direction when an external field is applied in the y_3-direction) is larger for Structure S_1 than for Structure S_2. This is expected and is attributed to the geometry of the unit cells. Fig. 6 refers to structure S_1 with some actuators/reinforcements oriented entirely in the y_3 direction. Fig. 7 refers to structure S_2 where none of the reinforcements are oriented in the y_3-direction (all 3 actuators/reinforcements are oriented at about 34° to the y_3 axis). Consequently, the stress response of structure S_2 in the y_1 direction when a voltage is applied in the y_3 direction is smaller and so is the corresponding effective coefficient $\tilde{P}_{113}$.

It is also of interest to analyze the variation of the effective coefficients of the structure S_2 vs. the angle of inclination of the actuators/reinforcements to the y_3 axis. As this angle increases, the actuators/reinforcements are oriented progressively closer to y_1- and y_2-axes, and, consequently, further away from the y_3-axis. Thus, one expects a corresponding increase in the values of effective coefficients, as it is seen in the Fig. 8 plotting $\tilde{P}_{113}$ and $\tilde{P}_{223}$.

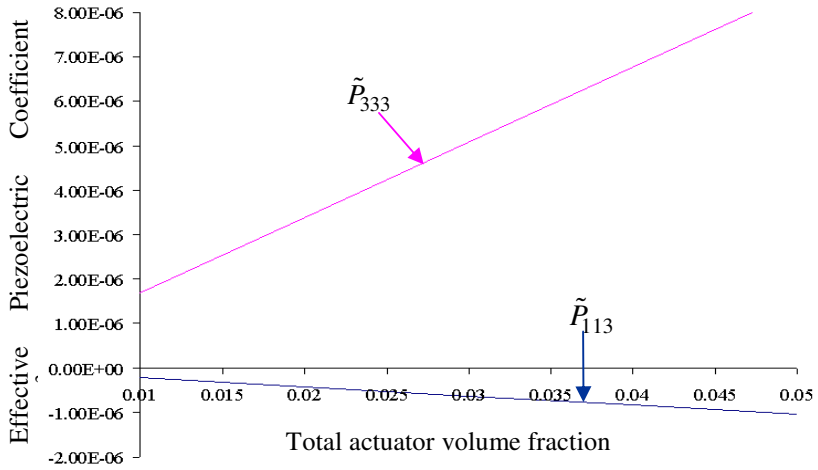

Figure 6. Plot of $\tilde{P}_{113}$ and $\tilde{P}_{333}$ effective piezoelectric coefficients vs. actuator volume fraction for structure S_1.

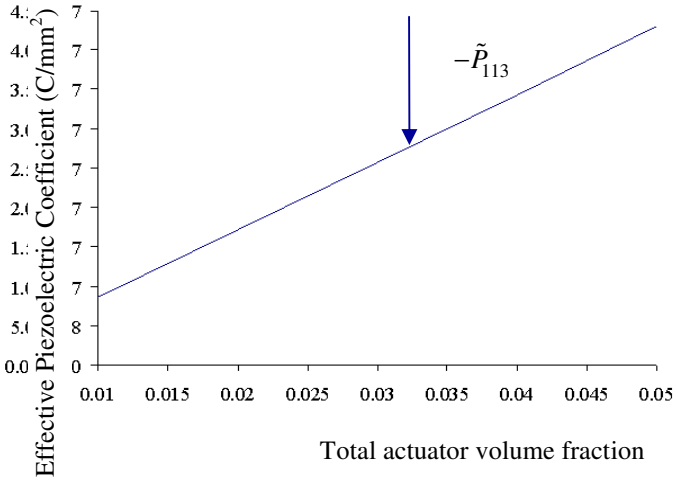

Figure 7. Plot of $-\tilde{P}_{113}$ effective piezoelectric coefficient vs. actuator volume fraction for structure S_2 (actuators oriented at 33.7° to the y_3 axis).

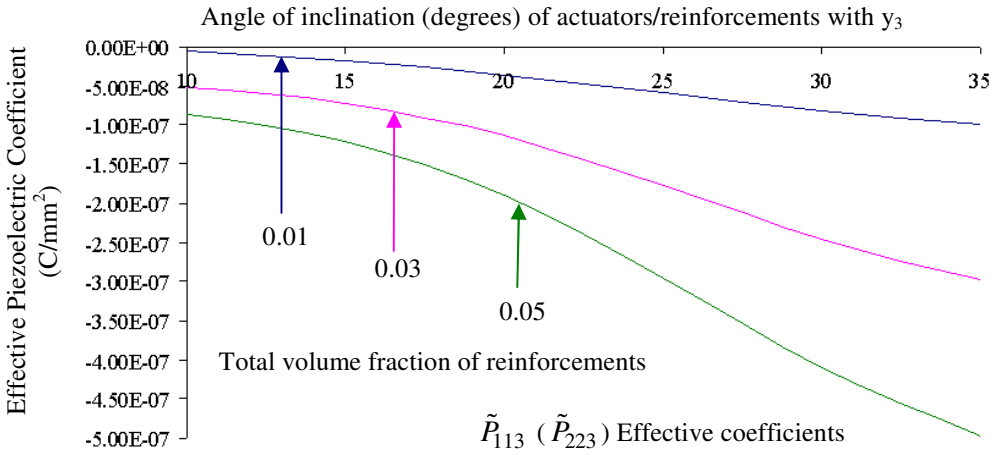

Figure 8. Plot of $\tilde{P}_{113}$ ($= \tilde{P}_{223}$) effective piezoelectric coefficient vs. inclination of actuators/reinforcements with the y_3 axis for different volume fractions (structure S_2).

We now turn our attention to structure S_3 shown in Fig. 5 and we will present graphically some of the effective piezoelectric coefficients vs. the relative height of the unit cell, see Fig. 9. The relative height is defined as the ratio of the height to the length of the unit cell. The width of the unit cell and the cross-sectional area of the reinforcements/actuators stay the same. It is noted that when the relative height of the unit cell is increased the total volume fraction of the reinforcements/actuators as well as the orientation angle between these actuators and y_3-axis will decrease. This has very interesting consequences on the effective coefficients. In particular, decrease of the angle of inclination of the actuators with the y_3-axis will reduce the stiffnesses in y_1 and y_2 directions because the actuators are oriented further away from the y_1-y_2 plane. The simultaneous decrease in the overall actuator volume fraction makes this effect even more pronounced. These trends are clearly visible in Fig. 9 for the coefficients $\tilde{P}_{112}$ and $\tilde{P}_{222}$.

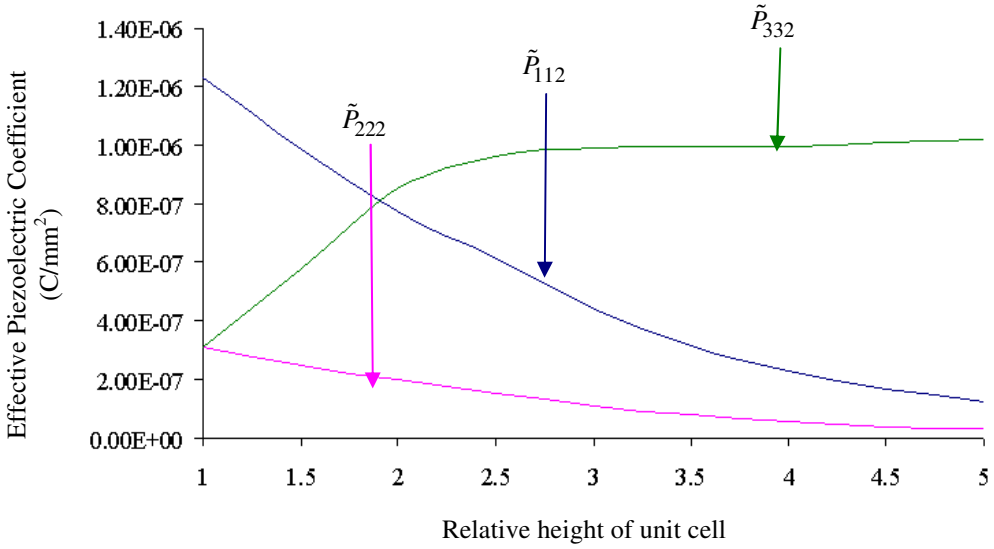

Figure 9. Plot of $\tilde{P}_{112}$, $\tilde{P}_{222}$, and $\tilde{P}_{332}$ effective piezoelectric coefficients vs. relative height of unit cell for structure S_3.

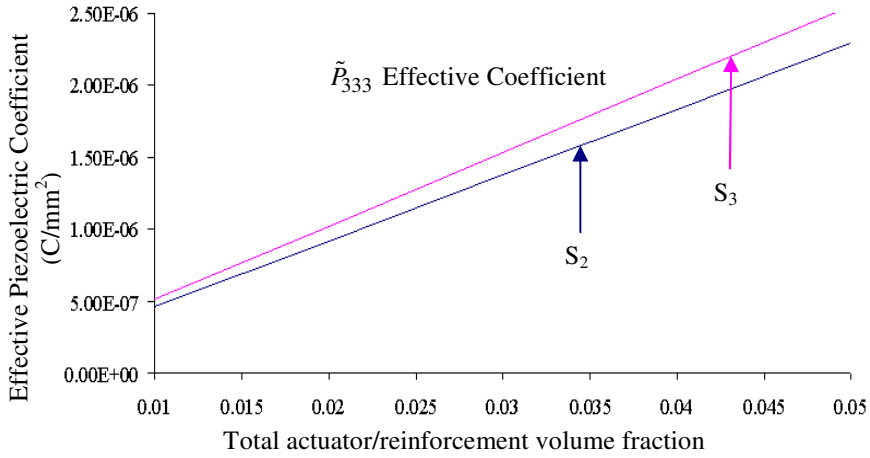

Figure 10. Plot of $\tilde{P}_{333}$ effective piezoelectric coefficient vs. total volume fraction for structures S_2 and S_3.

Finally, we compare the typical effective coefficients of structures S_2 and S_3 by varying the total volume fraction of the actuators/reinforcements but keeping the same dimensions of the respective unit cells, see Fig. 10. In conclusion, it is worth to mention that the developed micromechanical model allows the designer to develop a smart composite structure with the desirable combination of effective properties via selection of relevant material and geometric parameters such as number, type and cross-sectional dimensions of the actuators/reinforcements, relative dimensions of the unit cell, and the spatial orientation of the actuators/reinforcements. We also note that the advantage of our model is that the effective coefficients can be computed easily without the need of time consuming numerical (such as finite element) calculations.

6. ACKNOWLEDGEMENTS

The authors acknowledge the support of the Natural Sciences and Engineering Research Council of Canada (NSERC), and the Brazilian Research Agencies CNPq, FAPERJ and the National Institute of Science and Technology on Smart Structures for Engineering (INCT-EIE). The support of the Air Force Office of Scientific Research (AFOSR) is also acknowledged.

7. REFERENCES

Bakhvalov, N.S. and Panasenko, G.P., 1989, Averaging Processes in Periodic Media. Mathematical Problems in Mechanics of Composite Materials, Kluwer, Dordrecht.

Challagulla, K.S., Georgiades, A.V. and Kalamkarov, A.L., 2007. "Asymptotic homogenization modeling of thin network structures". Composite Structures, Vol. 3, pp. 432 – 444.

Challagulla, K.S., Georgiades, A.V., Saha, G.C. and Kalamkarov, A.L., 2008. "Micromechanical analysis of grid-reinforced thin composite generally orthotropic shells". Composites Part B: Engineering, Vol. 39, pp. 627 – 644.

Cote, F., Masson, P. and Mrad, N., 2002, "Dynamic and static assessment of piezoelectric embedded composites", Proceedings of the SPIE, Vol. 4701, pp. 316 – 325.

Georgiades, A.V., Challagulla, K.S. and Kalamkarov, A.L., 2006. "Modeling of the thermopiezoelastic behavior of prismatic smart composite structures made of orthotropic materials." Composites Part B: Engineering, Vol. 37, pp. 569 – 582.

Hassan, E.M., Georgiades, A.V., Savi, M.A. and Kalamkarov, A.L., 2011. "Analytical and numerical analysis of 3D grid-reinforced orthotropic composite structures." International Journal of Engineering Science.

Kalamkarov, A.L., 1992, Composite and Reinforced Elements of Construction, Wiley, Chichester, N.Y.

Kalamkarov, A.L., Andrianov, I.V. and Danishevs'kyy, V.V., 2009a. "Asymptotic homogenization of composite materials and structures." Transactions of the ASME, Applied Mechanics Reviews, Vol. 62, No. 3, pp. 030802-1 – 030802-20.

Kalamkarov, A.L. and Georgiades, A.V., 2002a. "Modeling of smart composites on account of actuation, thermal conductivity and hygroscopic absorption." Composites Part B: Engineering, Vol. 33, pp. 141 – 152.

Kalamkarov, A.L. and Georgiades, A.V., 2002b. "Micromechanical modeling of smart composite structures." Smart Materials and Structures, Vol. 11, pp. 423 – 434.

Kalamkarov, A.L. and Georgiades, A.V., 2004. "Asymptotic homogenization models for smart composite plates with rapidly varying thickness. Part. I. Theory." International Journal for Multiscale Computational Engineering, Vol. 2, Issue 1, pp. 133–148.

Kalamkarov, A.L., Georgiades, A.V., Challagulla, K.S. and Saha, G.C., 2006. "Micromechanics of smart composite plates with periodically embedded actuators and rapidly varying thickness". Journal of Thermoplastic Composite Materials, Special Issue on Smart Composites, Vol. 19, No. 3, pp. 251 – 276.

Kalamkarov, A.L., Hassan, E.M., Georgiades, A.V., Savi, M.A., 2009b. "Asymptotic homogenization model for 3D grid-reinforced composite structures with generally orthotropic reinforcements". Composite Structures, Vol. 89, No. 2, pp. 186 – 196.

Kalamkarov, A.L. and Kolpakov, A.G., 1997, Analysis, Design and Optimization of Composite Structures, Wiley, Chichester, N.Y.

Kalamkarov, A.L. and Kolpakov, A.G., 2001. "A new asymptotic model for a composite piezoelastic plate." International Journal of Solids and Structures, Vol. 38, No. 34-35, pp. 6027 – 6044.

Saha, G.C. and Kalamkarov, A.L., 2009. "Micromechanical thermoelastic model for sandwich composite shells made of generally orthotropic materials." Sandwich Structures and Materials, Vol. 11, No. 1, pp. 27 – 56.

Saha, G.C., Kalamkarov, A.L. and Georgiades, A.V., 2007a. "Effective elastic characteristics of honeycomb sandwich composite shells made of generally orthotropic materials." Composites Part A: Applied Science and Manufacturing, Vol. 38, No. 6, pp. 1533–1546.

Saha, G.C., Kalamkarov, A.L. and Georgiades, A.V., 2007b. "Micromechanical analysis of effective piezoelastic properties of smart composite sandwich shells made of generally orthotropic materials." Smart Materials and Structures, Vol. 16, pp. 866 – 883.

Sanchez-Palencia, E., 1980, Non-homogeneous Media and Vibration Theory, Springer, Berlin, N.Y.

8. RESPONSIBILITY NOTICE

The authors are the only responsible for the printed material included in this paper.